DOI 10.1007/s10778-017-0801-y
International Applied Mechanics, Vol. 53, No. 2, March, 2017

LOSS OF STABILITY IN A COMPOSITE LAMINATE COMPRESSED BY A SURFACE LOAD

V. M. Bystrov, V. A. Dekret, and V. S. Zelenskii

The critical loads for a layered material compressed by a surface load are determined numerically using the three-dimensional linearized theory of stability and the piecewise-homogeneous material model. Symmetry conditions on the lateral sides of a layered composite sample are assumed. It is shown that internal loss of stability in the layered composite is microbuckling near the loaded surface manifested as end crushing. The buckling modes decay with distance from the end. The effect of the inhomogeneity of the initial state induced by the load on the buckling modes is studied. The inhomogeneity of the initial state has a strong effect on the amplitudes of the buckling modes and the area of their localization

Keywords: layered composite material, uniaxial longitudinal compression, surface load, buckling mode, three-dimensional linearized theory of stability, end crushing, inhomogeneity of initial state

Introduction. Mechanical loads on structural members made of composite materials are usually directed along reinforcements. The strength characteristics of composites in compression and tension differ substantially and are very difficult to predict under compression. This motivates studies on the mechanics of composites compressed [2–4, 13, 24, 26, 30]. Compressive stresses may cause loss of stability and fracture of composites at macro- and micro-scales. One of the main failure mechanisms in fibrous and laminated composites under compression is microbuckling [2–4, 7, 13–15, 17–19, 22, 24, 26, 27, 29–32]. Some analytical and numerical results on the behavior of compressed unidirectional composites subject to this type of failure mechanism are analyzed in [26]. The Rosen model [29] was the earliest and is the most cited. This pioneering publication was analyzed in detail in [3, 4, 22]. We will show qualitative contradictions and quantitative errors related to this model compared with the three-dimensional linearized theory of stability of deformable bodies (TLTSDB) [1, 16]. The TLTSDB is the most exact, rigorous, and consistent in solid mechanics.

As shown in [2], the failure mechanism of a composite longitudinally compressed by a surface load may be near-surface buckling near the loaded end of the composite specimen, with buckling modes decaying with distance from that end. Nonclassical problems of fracture mechanics were formulated in [3, 17, 20]. End crushing of composite specimens and structural members under compression is considered one of such nonclassical problems. This problem was first formulated in [3, 17, 20] as a separate research area of the fracture mechanics of composites.

The continuum theory of end crushing was addressed in [2]. According to this theory, the brittle fracture of a composite with nonclampled ends under uniaxial compression is described as follows [2, p. 581]: “First, the ends are crushed and surface fracture occurs near free lateral surfaces under an external load slightly lower than the minimum reduced shear modulus. As the external load becomes equal to the minimum reduced shear modulus, internal fracture occurs spreading avalanche-like over surfaces, almost perpendicularly to the direction of the external load.” By nonclamped ends are meant the case where end crushing is intentionally not excluded.

S. P. Timoshenko Institute of Mechanics, National Academy of Sciences of Ukraine, 3 Nesterova St., Kyiv, Ukraine 03057, e-mail: numer@inmech.kiev.ua. Translated from Prikladnaya Mekhanika, Vol. 53, No. 2, pp. 49–58, March–April, 2017. Original article submitted July 4, 2016.

The numerical results on the near-surface buckling of an under-reinforced laminate in piecewise-homogeneous subcritical state under uniaxial surface loading obtained in [7, 23] using a piecewise-homogeneous material model confirm the presence of such a failure mechanism.

The problem of the stability of a laminated composite uniaxially compressed by a surface load was numerically solved in [6, 12] using the piecewise-homogeneous material model. The composite was represented by a two-layer model with symmetry conditions on its lateral faces. The case of inhomogeneous subcritical state related to the constraints on displacements in the end plane and the complex loading conditions on the surface (the surface load is applied only to the reinforcement and, generally, has a spatial period comparable to or exceeding the typical length scale of the material. The size and geometry of the inhomogeneity region of the stress state, the distribution of stresses and strains depend on the ratio of the mechanical and geometrical characteristics of the composite components, the degree of their anisotropy, and the ratio of geometrical parameters that define the microstructure of the composite and the size of the model [11, 25]. Nonzero shear stresses in the region of application of the surface load are known to have a strong effect on the stability-critical parameters of the composite [27, 32]. The inhomogeneity of the subcritical state also affects the microbuckling failure mechanisms, their sequence, and interaction in structural members and specimens made of composites.

Here we will use the TLTSDB equations, which take into account the inhomogeneity of the initial state, and the piecewise-homogeneous material model to study the near-surface buckling of unidirectional composite laminate compressed by a surface load along the plies. We will consider an inhomogeneous initial state induced by a load applied to the reinforcement and a piecewise-homogeneous state induced by a statically equivalent surface load applied to the reinforcement and matrix and leading to a homogeneous stress–strain state in the reinforcement and matrix. We will study the influence of the inhomogeneity of the initial state on the buckling modes of a composite laminate for two-layer models with symmetry conditions on the sides and different concentrations of reinforcement.

Since it is difficult to find analytic solutions to problems of this class, modern numerical methods have to be used [5, 8, 9]. We will use a mesh-based method based on the modified variational difference approach [5]. This approach to analyzing the stability of fibrous and laminated composites in inhomogeneous subcritical states was developed in [4, 6, 10–12, 22].

1. Problem Statement. Design Models. Consider a laminated two-component composite of regular structure (Fig. 1*a*) for two loading configurations. One loading configuration is uniform uniaxial compression of reinforcement plies by surface load of constant intensity ((1) in Fig. 1*a*) that induces an inhomogeneous subcritical state.

The surface load p_1 acts along the Ox_2-axis and is applied to the reinforcement plies:

$$p_1(x_1) = \sigma_{22}(x_1, 0) = p^0, \qquad |x_1| \le h_\mathrm{r} / 2 + kb, \qquad k = 0, 1, \ldots . \tag{1.1}$$

The spatial period b of the surface load is equal to the spatial period of the composite structure: $b = h$, $h = h_\mathrm{r} + h_\mathrm{m}$, where h_r and h_m are the thicknesses of the reinforcement and matrix plies, respectively. The load does not vary along the Ox_3-axis. The other loading configuration is uniform uniaxial compression of the reinforcement and matrix plies by surface loads of constant intensity that induce a homogeneous stress state ((2) in Fig. 1*a*). These loads are determined in computational experiment using the first loading configuration. They are the normal stresses σ_{22}^r, σ_{22}^m in the reinforcement and matrix far from the line of application of the surface load along the Ox_2-axis. Such an experiment involves an analysis of the decay of the edge effect in compressed reinforcement plies [11, 25]. For the second loading configuration, we, thus, have

$$p_2(x_1) = \sigma_{22}^\mathrm{r}(x_1, x_2 = \lambda) = p_\mathrm{r}^0, \qquad |x_1| \le h_\mathrm{r} / 2 + kb,$$

$$p_2(x_1) = \sigma_{22}^\mathrm{m}(x_1, x_2 = \lambda) = p_\mathrm{m}^0, \qquad |x_1| \le (h_\mathrm{r} / 2 + h_\mathrm{m}) + kb,$$

$$k = 0, 1, \ldots, \tag{1.2}$$

where λ is the edge-effect length determined with accuracy sufficient for our calculations. At infinity, the reinforcement plies are compressed too. Since the load is symmetric and the structure of the composite is regular, the buckling problem can be solved using finite models. We will use a two-layer model shown in Fig. 1 to study the influence of the inhomogeneity of the initial state on the near-surface buckling of the composite. The boundary conditions on the sides of the model are symmetry conditions. As shown in [6, 12], such a model can be used to study near-surface buckling during end crushing. It is well to bear in mind that, as indicated in [12], the critical loads will be higher than for design models of a composite with periodic structure. This is due to

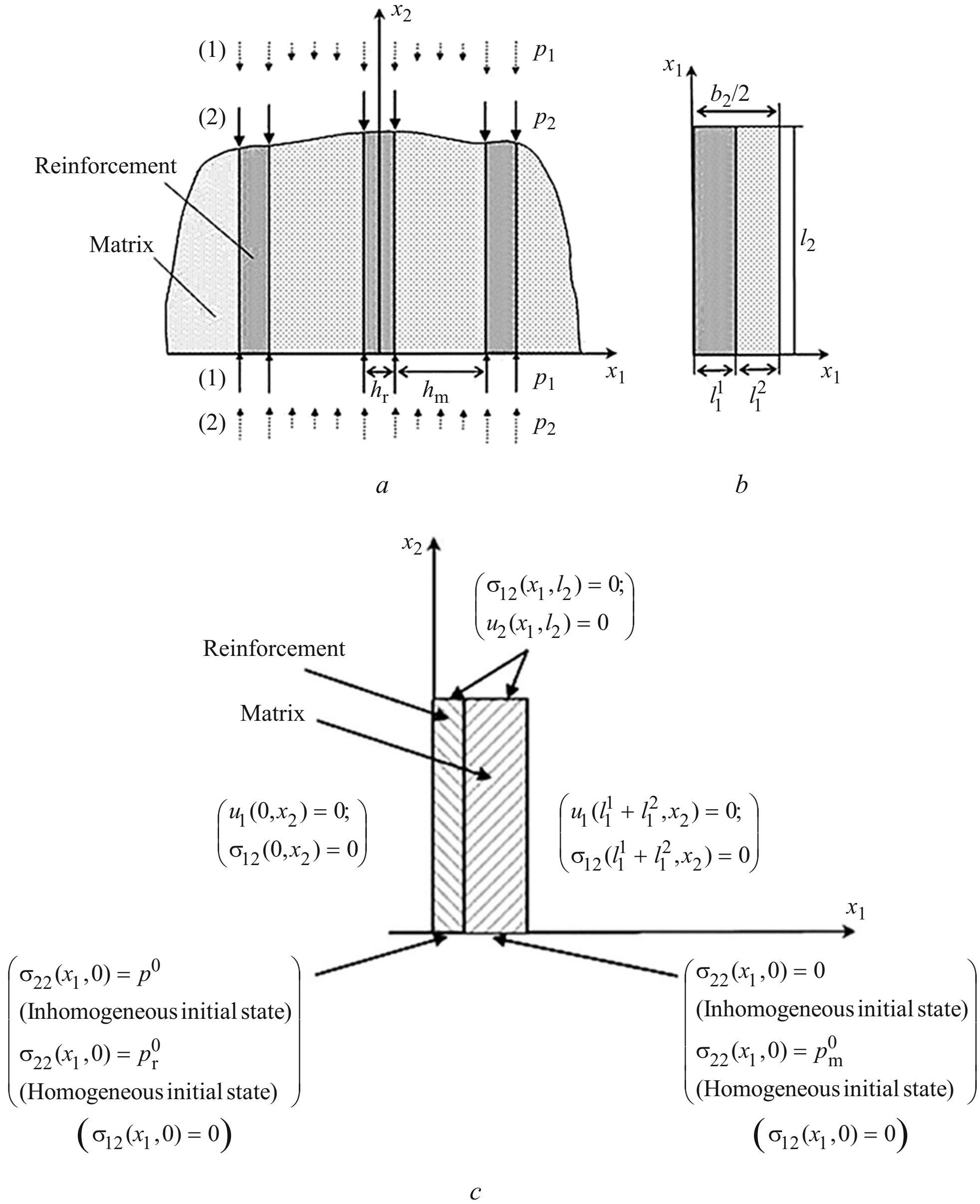

Fig. 1

additional constraints such as mixed boundary conditions on the lateral sides of the model, which correspond to the symmetry conditions and include kinematic conditions for one of the components.

Thus, we will use two design models to compare the microbuckling of the material in inhomogeneous and homogeneous initial states.

Let the load be a dead one, which is sufficient for applicability of the static TLTSDB method [18]. We will use this static method and the second theory of small subcritical deformations, assuming that the matrix and reinforcement are quite stiff. The subcritical state can be determined by solving the problem of linear elasticity for piecewise-homogeneous bodies.

In formulating the problem, we will use a Cartesian coordinate system $Ox_1x_2x_3$ and place the composite in the upper half-space $x_2 \geq 0$. Let the plies extend along the Ox_3-axis, be parallel to the plane Ox_2x_3, and let the surface compressive load act along the Ox_2-axis. If these conditions are satisfied, the problem can be formulated as two-dimensional for plane strain in the plane x_1Ox_2 (Fig. 1). Thus, we deal with a boundary-value problem with boundary conditions represented by the loading conditions (1.1) and (1.2) shown in Fig. 1.

If Euler's static method is used, the buckling problem is reduced to a generalized eigenvalue problem in which the minimum eigenvalue is the critical load and the associated eigenfunction describes the buckling mode. The equations and boundary conditions for determining the critical loads of the composite structures are

$$(\sigma_{im} + \mu\sigma^0_{ik} u_{m,k})_{,i} = 0, \quad x \in \Omega, \tag{1.3}$$

$$(\sigma_{21} + \mu\sigma^0_{2k} u_{1,k}) = 0 \wedge u_2 = 0, \quad x \in S_1,$$

$$(\sigma_{12} + \mu\sigma^0_{1k} u_{2,k}) = 0 \wedge u_1 = 0, \quad x \in S_2,$$

$$(\sigma_{im} + \mu\sigma^0_{ik} u_{m,k}) = 0, \quad x \in S_3,$$

$$(\sigma_{22} + \mu\sigma_{22} u_{2,2}) = 0, \quad x \in S_4,$$

$$(\sigma_{12} + \mu\sigma^0_{1k} u_{2,k}) = 0 \wedge u_1 = 0, \quad x \in S_5. \tag{1.4}$$

The interface conditions between plies are

$$[\sigma_{ij}] = 0, \quad [u_i] = 0. \tag{1.5}$$

The critical load is determined from the following conditions:

$$p_{\text{cr}} = \min|\mu|/(l_1^1 + l_1^{21}) \int_{x_1 \in S_3 \cup S_4} p(x_1)\, dx_1 = \min|\mu|\, p^0 l_1^1 / (l_1^1 + l_1^2), \tag{1.6}$$

$$p_{\text{cr}} = \min|\mu|/(l_1^1 + l_1^{21}) \int_{x_1 \in S_3 \cup S_4} p(x_1)\, dx_1 = \min|\mu|(p_{\text{r}}^0 l_1^1 + p_{\text{m}}^0 l_1^2)/(l_1^1 + l_1^2), \tag{1.7}$$

where $\min|\mu|$ is the minimum (in absolute magnitude) eigenvalue of problem (1.3)–(1.5). The form of (1.6) reflects the fact that the compressive load is applied only to the reinforcement plies. Formula (1.7) corresponds to the case where the load is applied to both reinforcement and matrix plies.

The subcritical state is determined from the equations of linear elasticity, which together with the boundary conditions and the constitutive relations, have the form

$$\sigma^0_{ij,i} = 0, \quad x \subset \Omega,$$

$$\sigma^0_{21} = 0 \wedge u^0_2 = 0, \quad x \in S_1,$$

$$\sigma^0_{12} = 0 \wedge u^0_1 = 0, \quad x \in S_2,$$

$$\sigma^0_{ij} = 0, \quad x \in S_3,$$

$$\sigma^0_{22} = p^0 \wedge \sigma^0_{21} = 0, \tag{1.8}$$

$x \in S_4$ is inhomogeneous initial state;

$$\sigma^0_{22} = p^0_{\text{m}} \wedge \sigma^0_{21} = 0, \quad x \in S_3,$$

$$\sigma^0_{22} = p^0_{\text{r}} \wedge \sigma^0_{21} = 0, \quad x \in S_4$$

is homogeneous initial state;

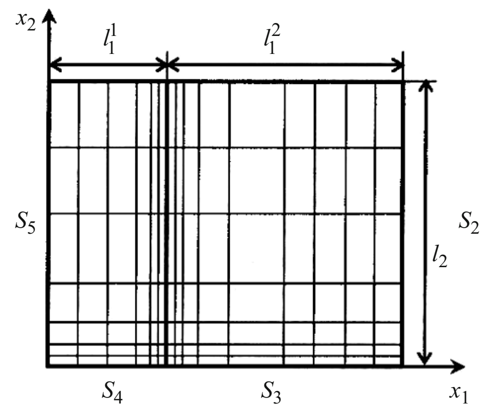

Fig. 2

$$\sigma_{12}^0 = 0 \wedge u_1^0 = 0, \quad x \in S_5, \tag{1.9}$$

$$\sigma_{ii}^0 = A_{ik}\varepsilon_{ik}, \quad \sigma_{ij}^0 = 2G\varepsilon_{ij}, \quad \varepsilon_{ij} = 0.5(u_{i,j} + u_{j,i}), \quad i \neq j, \tag{1.10}$$

$$A_{ii} = \frac{E(1-\nu)}{(1+\nu)(1-2\nu)}, \quad A_{ij} = \frac{E\nu}{(1+\nu)(1-2\nu)}. \tag{1.11}$$

Notation in (1.3)–(1.11) is standard, the indices change from 1 to 2, and "$\wedge$" and "$\vee$" are the conjunction and disjunction signs. In (1.3)–(1.9), the superscript "0" refers to the subcritical state. The index referring to a ply of the composite structure is omitted for convenience. The following notation is used for the boundaries of the models:

$$S_1 \in \left(0 \le x_1 \le (l_1^1 + l_1^2) \wedge x_2 = l_2\right), \quad S_2 \in \left(x_1 = (l_1^1 + l_1^2) \wedge 0 \le x_2 \le l_2\right),$$

$$S_3 \in \left(l_1^1 \le x_1 \le (l_1^1 + l_1^2) \wedge x_2 = 0\right), \quad S_4 \in (0 \le x_1 \le l_1^1 \wedge x_2 = 0),$$

$$S_5 \in (x_1 = 0 \wedge 0 \le x_2 \le l_2).$$

To compare the critical loads and buckling modes in the composite for homogeneous and inhomogeneous subcritical states, the stationary inhomogeneous subcritical stresses are determined by conducting a computational experiment. These loads are used at the subsequent stages of the computational experiment to set loading conditions that lead to a piecewise-homogeneous subcritical state.

2. Numerical Solution. Problem (1.3)–(1.6) is solved by the mesh-based method using the concept of base scheme. With such an approach, the difference scheme for the computational domain is constructed at each node as a sum of values of the base scheme, which is a difference scheme obtained by a variational difference method for the cell template of the difference mesh [5].

For numerical purposes, the problem for the original semi-infinite model of the composite is reduced to a problem for a finite model. The size of this model is determined in a computational experiment from the condition that the parameters no longer change with increase in the dimension of the domain along the Ox_2-axis. Such parameters are the critical loads and the size of the region in which the subcritical state is inhomogeneous.

Figure 2 shows the design model covered by a nonuniform difference mesh. Over the rectangular nonuniform difference mesh $\overline{\omega} = \omega + \gamma$, which approximates the domain $\overline{\Omega}$, problem (1.3)–(1.6) is associated with the following difference problem:

$$A_m \boldsymbol{u} = \mu B_m \boldsymbol{u}, \quad \boldsymbol{x} \in \overline{\omega} \tag{2.1}$$

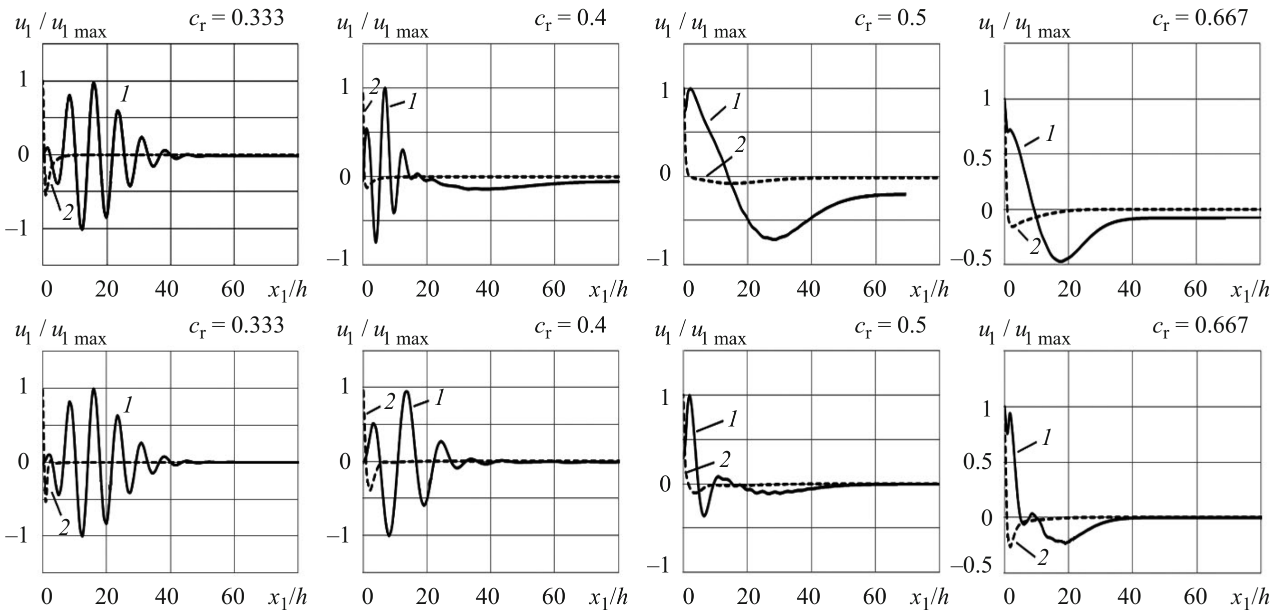

a *b* *c* *d*

Fig. 3

$$\left[A_m \boldsymbol{u} = \begin{cases} \sum\limits_{\xi \in x} a_m(\xi)\boldsymbol{u}, & \boldsymbol{x} \in \bar{\omega} - \gamma_{u_m}, \\ Eu_m, & \boldsymbol{x} \in \gamma_{u_m}, \end{cases} \qquad B_m \boldsymbol{u} = \begin{cases} \sum\limits_{\xi \in x} b_m(\xi)\boldsymbol{u}, & \boldsymbol{x} \in \bar{\omega} - \gamma_{u_m}, \\ Eu_m, & \boldsymbol{x} \in \gamma_{u_m}, \end{cases} \right.$$

$$a_i(\xi)u = -H \frac{\sigma_{ji} + \sigma_{ji}^{\xi_j}}{\eta_{\xi_j}}, \qquad b_i(\xi)u = -H \frac{\sigma_{jk}^0 u_{i,\xi_k} + (\sigma_{jk}^0 u_{i,\xi_k})^{\xi_j}}{\eta_{\xi_j}}, \quad \boldsymbol{x} \in \bar{\omega},$$

$$\left. \sigma_{ii} = A_{ik}\varepsilon_{kk}, \quad \sigma_{12} = 2G\varepsilon_{12}, \quad \varepsilon_{ij} = 0.5(u_{i,\xi_j} + u_{j,\xi_i}), \quad z_{,\xi_i} = -\mathrm{sign}(\xi_i)\frac{z^{-\xi_i} - z}{h_i} \right], \tag{2.2}$$

where the variables are denoted (wherever possible) in the same manner as the respective continuum variables, which would hardly lead to a misunderstanding; a_m and b_m are the components of the base operators $\boldsymbol{a}$ and $\boldsymbol{b}$; H is the cell area; h_i is the size of the cell in the x_i-direction; σ_{ij} and ε_{ij} are difference analogs of the stresses and strains in (1.3)–(1.7); $z_{,\xi_i}$ is the difference derivative of the mesh function $z(\xi)$ in the x_i-direction (right derivative for $\xi_i < 0$); $\xi = (\xi_1, \xi_2)$, $\xi_i = \pm i$ is the node parameter of the cell; $\sum_{\xi \in x}$ denotes the summation of a component of the reference scheme over those parameters ξ that coincide with the mesh node $\boldsymbol{x}$; $\xi_{-i} = -\xi_i$; E is an identity operator, γ_{u_m} is the section of the boundary γ on which the mth component of the difference analog of the boundary condition is set for displacements.

The discrete problems are solved using effective numerical methods [28] and the following procedure outlined in [5]. The algebraic problem is solved with the direct Cholesky method. After the refinement of the difference mesh, the conjugate-gradient method is used. The solution found with the Cholesky method is interpolated and used as an initial approximation for solving the discrete eigenvalue problem by the subspace iteration method.

3. Analysis of the Numerical Results. Consider a laminated composite material surface loading conditions (1.1) and (1.2) and the following mechanical and geometric characteristics: $E^1 / E^2 = 100$, $\nu^1 = \nu^2 = 0.3$, $c_r = S_4 / (S_3 + S_4) = 0.333$, 0.4, 0.5, 0.667 (where c_i is the volume fraction of the reinforcement; E^1, E^2 and ν^1, ν^2 are, respectively, Young's moduli and Poisson's ratios of the reinforcement and matrix).

Figure 3 shows buckling modes $u_1(x_2)/u_1^{\max}$ in a reinforcement ply (left) and in a matrix ply (right) for different concentrations of reinforcement in sections x_1 / h corresponding to the maximum $u_1^{\max}$ of the displacement perturbations u_1. The coordinate x_2 is divided by $h = h_r + h_m$. Curves *1* correspond to inhomogeneous initial state, and curves *2* to homogeneous initial state.

It can be seen that the buckling modes are localized near the surface of the material and decay with distance from it. With increase in the volume fraction of the reinforcement, the buckling mode in the reinforcement and matrix plies decay differently. If the subcritical state is piecewise-homogeneous, the region where the buckling modes are localized is much smaller than in an inhomogeneous subcritical state.

Conclusions. 1. Representing the composite by a two-layer model with symmetry conditions on its sides allows studying the near-surface buckling during end crushing.

2. Microbuckling in a laminated composite material with a reinforcement volume fraction of 0.167–0.667 occurs near the loaded surface with buckling modes decaying with distance from the end. This indicates that microbuckling in a composite under uniaxial compression results in end-crushing failure.

3. The inhomogeneity of the subcritical state has a strong effect on the amplitudes of the buckling modes and the size of the region where they are localized. If the subcritical state is piecewise-homogeneous, the region where the buckling modes are localized is much smaller than in an inhomogeneous subcritical state.

REFERENCES

1. A. N. Guz, *Fundamentals of the Three-Dimensional Theory of Stability of Deformable Bodies* [in Russian], Vyshcha Shkola, Kyiv (1986).
2. A. N. Guz, *Fracture Mechanics of Compressed Composite Materials* [in Russian], Naukova Dumka, Kyiv (1990).
3. A. N. Guz, *Fundamentals of the Fracture Mechanics of Compressed Composites* [in Russian], in two vols., Litera, Kyiv (2008).
4. A. N. Guz and V. A. Dekret, *Short-Fiber Model in the Theory of the Stability of Composites* [in Russian], LAP Lambert Acad. Publ., SaarbrTimes New Roman CE”ъcken (2015).
5. Ya. M. Grigorenko, Yu. N. Shevchenko, A. T. Vasilenko, et al., *Numerical Methods*, Vol. 11 of the 12-volume series *Mechanics of Composite Materials* [in Russian], A.S.K., Kyiv (2002).
6. V. S. Zelenskii, V. A. Dekret, and V. M. Bystrov, “Stability of a composite laminate at uniaxial loading,” in: *Trans. Dniprodzerzhinsk State Technical University* [in Russian], Issue 2(19) (Mathematical Problems of Engineering Mechanics), DDTU, Dniprodzerzhinsk (2012), pp. 49–53.
7. Yu. V. Kokhanenko, “Brittle end-crushing failure of composites,” *Dokl. AN SSSR*, **296**, No. 4, 805–808 (1987).
8. J. E. Akin, *Finite Element Analysis Concepts: via SolidWorks*, World Scientific, Hackensack, NJ (2010).
9. E. J. Barbero, *Finite Element Analysis of Composite Materials Using ANSYS*, CRC Press (2013).
10. E. Yu. Bashchuk and V. Yu. Baichuk, “Influence of the principal stress state on the critical loads of a plate with a crack,” *Int. Appl. Mech.*, **49**, No. 3, 328–336 (2013).
11. V. M. Bystrov, V. A. Dekret, and V. S. Zelenskii, “Numerical analysis of the edge effect in a composite laminate with compressed reinforcement plies,” *Int. Appl. Mech.*, **51**, No. 5, 561–566 (2015).
12. V. A. Dekret, V. S. Zelenskii, and V. M. Bystrov, “Numerical analysis of stability of a laminated composite with uniaxially compressed reinforcement plies,” *Int. Appl. Mech.*, **50**, No. 5, 549–557 (2014).
13. N. A. Fleck, “Compressive failure of fiber composites,” *Adv. Appl. Mech.*, **33**, 43–117 (1997).
14. L. B. Greszczuk, “Microbuckling failure of lamina-reinforced composites,” in: *Proc. 3rd Conf Composite Materials: Testing and Design ASTM STP*, No. 546, Philadelphia (Pa) (1974), pp. 5–29.
15. L. B. Greszczuk, “Microbuckling failure of circular fiber-reinforced composites,” *AIAA J.*, **13**, 1311–1318 (1975).
16. A. N. Guz, *Fundamentals of the Three-Dimensional Theory of Stability of Deformable Bodies*, Springer-Verlag, Heilberg–Berlin (1999).
17. A. N. Guz, “On study of nonclassical problems of fracture and failure mechanics and related mechanisms,” *Int. Appl. Mech.*, **45**, No. 1, 1–31 (2009).
18. A. N. Guz, “Setting up a theory of stability of fibrous and laminated composites,” *Int. Appl. Mech.*, **45**, No. 6, 587–613 (2009).

19. A. N. Guz, “Stability of elastic bodies under uniform compression (review),” *Int. Appl. Mech.*, **48**, No. 3, 241–293 (2012).
20. A. N. Guz, I. A. Guz, A. V. Menshikov, and V. A. Menshikov, “Three-dimensional problems in the dynamic fracture mechanics of materials with interface cracks (review),” *Int. Appl. Mech.*, **49**, No. 1, 3–79 (2013).
21. A. N. Guz and V. A. Dekret, “On two models in three-dimensional theory of stability of composite materials,” *Int. Appl. Mech.*, **44**, No. 8, 839–854 (2008).
22. A. N. Guz and V. A. Dekret, “Finite-fiber model in the three-dimentional theory of stability of composites (review),” *Int. Appl. Mech.*, **52**, No. 1, 1–48 (2016).
23. A. N. Guz and Yu. V. Kokhanenko, “Numerical solution of three-dimentional stability problems for elastic bodies,” *Int. Appl. Mech.*, **37**, No. 11, 1369–1399 (2001).
24. P. M. Jelf and N. A. Fleck, “Compression failure mechanisms in unidirectional composites,” *J. Comp. Mater.*, **26**, No. 18, 2706–2726 (1992).
25. Yu. V. Kokhanenko and V. M. Bystrov, “Edge effect in a laminated composite with longitudionally compressed laminas,” *Int. Appl. Mech.*, **42**, No. 8, 922–927 (2006).
26. N. K. Naik and R. S. Kumar, “Compressive strength of unidirectional composites: evaluation and comparison of prediction models,” *Compos. Struct.*, **46**, 299–308 (1999).
27. M. D. Nestorovic and N. Triantafyllidis, “Onset of failure in finitely strained layered composites subjected to combined normal and shear loading,” *J. Mech. Phys. Solids*, **52**, 941–974 (2004).
28. S. Pissanetzky, *Sparse Matrix Technology*, Academic Press, London (1984).
29. B. W. Rosen, “Mechanics of composite strengthening,” in: *Fiber Composite Materials*, *American Society of Metals*, Metals Park, OH (1965), pp. 37–75.
30. C. Soutis, *Compressive Behavior of Composites*, Rapra Technology Ltd, United Kingdom (1997).
31. N. Triantafyllidis and W.C. Scynaidt, “Comparison of microscopic and macroscopic instabilities in a class of two-dimensional periodic composites,” *J. Mech. Phys. Solids*, **41**, No. 9, 1533–1565 (1993).
32. T. J. Vogler, S.-Y. Hsu, and S. Kyriakides, “Composite failure under combined compression and shear,” *Int. J. Solids Struct.*, **37**, No. 12, 1765–1791 (2000).